













Severe decline in large farmland trees in India over the past decade

Received: 29 September 2023

Accepted: 19 April 2024

Published online: 15 May 2024

 Check for updates

Martin Brandt ^{1,5} , Dimitri Gominski ^{1,5} , Florian Reiner ^{1,5} , Ankit Kariryaa ^{1,2}, Venkanna Babu Guthula², Philippe Ciais ³, Xiaoye Tong ¹, Wenmin Zhang ¹, Dhanapal Govindarajulu ⁴, Daniel Ortiz-Gonzalo¹ & Rasmus Fensholt ¹

Agroforestry practices that include the integration of multifunctional trees within agricultural lands can generate multiple socioecological benefits, in addition to being a natural climate solution due to the associated carbon sequestration potential. Such agroforestry trees represent a vital part of India's landscapes. However, despite their importance, a current lack of robust monitoring mechanisms has contributed to an insufficient grasp of their distribution in relation to management practices, as well as their vulnerability to climate change and diseases. Here we map 0.6 billion farmland trees, excluding block plantations, in India and track them over the past decade. We show that around $11 \pm 2\%$ of the large trees (about 96 m^2 crown size) mapped in 2010/2011 had disappeared by 2018. Moreover, during the period 2018–2022, more than 5 million large farmland trees (about 67 m^2 crown size) have vanished, due partly to altered cultivation practices, where trees within fields are perceived as detrimental to crop yields. These observations are particularly unsettling given the current emphasis on agroforestry as a pivotal natural climate solution, playing a crucial role in both climate change adaptation and mitigation strategies, in addition to being important for supporting agricultural livelihoods and improving biodiversity.

Wildfires, fungi, insects and droughts cause considerable tree mortality in forests and other forested ecosystems¹. Anthropogenic climate change, human appropriation and mismanagement are further aggravating tree die-offs, which have reached alarming levels in recent years^{2,3}. These events are well documented, and the public awareness is high because operational monitoring systems based on satellites are able to locate and quantify forest diebacks and deforestation¹. However, only little is known on potential widespread diebacks and human appropriation of trees outside forests, such as in drylands or trees on farms. Agroforestry is a land-use practice that integrates multifunctional trees in agricultural land to maximize socioecological

benefits from trees⁴. Agroforestry trees have drawn a lot of interest in relation to tree planting and restoration as an underexplored pathway towards climate mitigation, but little attention is paid to the protection of existing on-farm trees in mature agroforestry systems and how they are being affected by the mentioned threats.

According to a recent state-of-the-art land-cover map⁵, 56% of India is covered by farmland, and only 20% is covered by forest. While the separation of forests and tree plantations is not always clear, it is unequivocal that these classifications exclude a large part of India's trees, which are scattered within farmlands, in urban areas or grown as hedgerows^{6,7}. These multipurpose trees, such as *Prosopis cineraria*,

¹Department of Geosciences and Natural Resource Management, University of Copenhagen, Copenhagen, Denmark. ²Department of Computer Science, University of Copenhagen, Copenhagen, Denmark. ³Laboratoire des Sciences du Climat et de l'Environnement, CEA/CNRS/UVSQ/Université Paris Saclay, Gif-sur-Yvette, France. ⁴Global Development Institute, University of Manchester, Manchester, UK. ⁵These authors contributed equally: Martin Brandt, Dimitri Gominski, Florian Reiner. ✉e-mail: mabr@ign.ku.dk; dg@ign.ku.dk; fr@ign.ku.dk

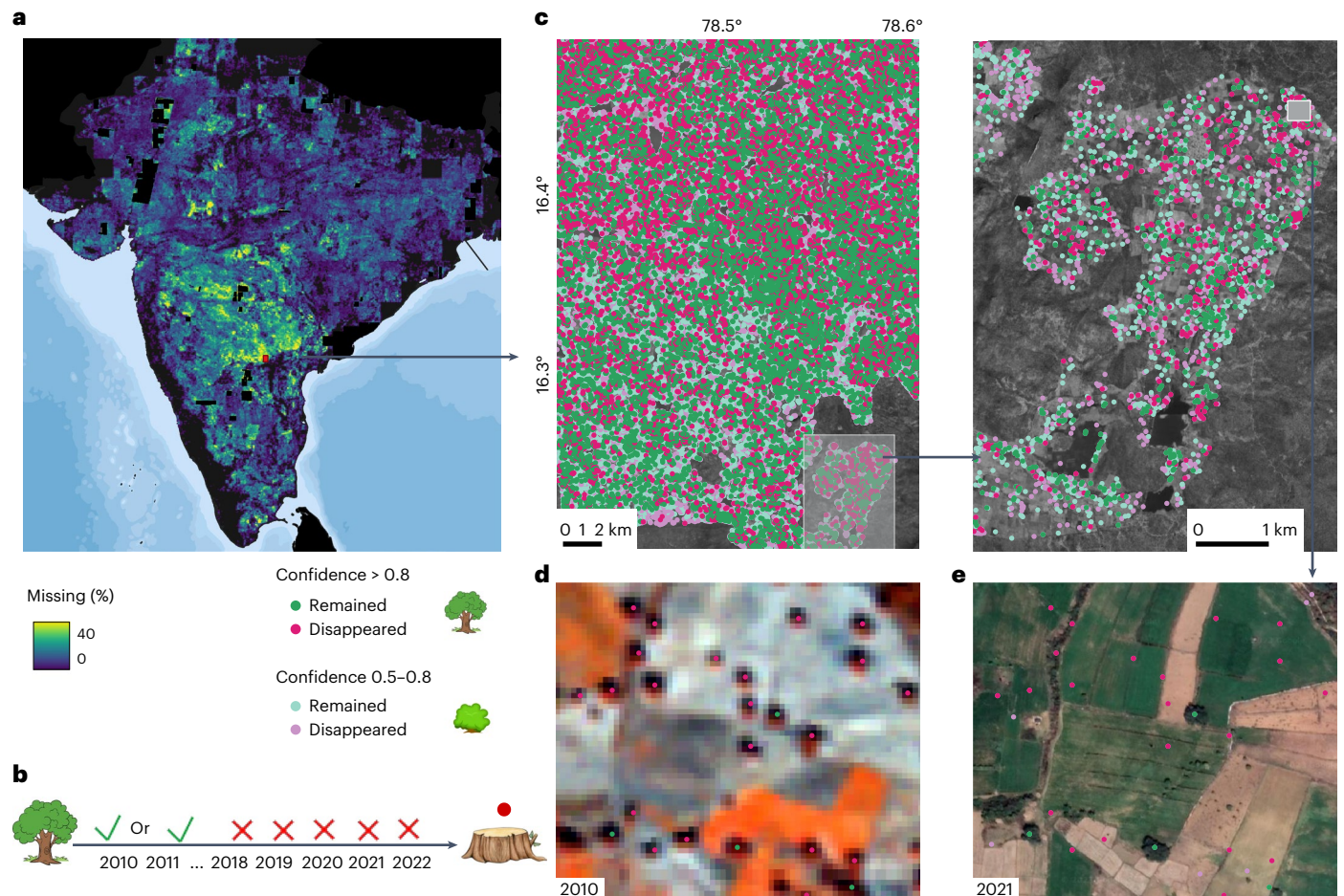


Fig. 1 | Severe losses in large agroforestry trees 2010–2018. India has experienced massive losses of large farmland trees, illustrated here at the tree level tracked with RapidEye (2010/2011) and PlanetScope (2018–2022). **a**, Trees that have disappeared are shown here as a percentage in relation to the total number of mapped trees in 2010 aggregated to 5×5 km grids. **b**, A tree detected in either 2010 or 2011 but not during 2018–2022 was classified as disappeared. If a tree mapped in 2010/2011 was observed in any of the years between 2018 and 2022, it was classified as remained. **c**, Trees mapped with RapidEye have an average crown area of 96 m^2 (confidence >0.8 ; Methods). Many regions have

lost up to half of these large trees within farmlands during 2010–2018 (note that only trees in farmlands are considered, using WorldCover as a mask layer). The rectangle marks the area of the close-up, and the arrow shows the location within India. **d**, Trees mapped with RapidEye in 2010, shown here as a false colour composite. **e**, The same area in 2021 is illustrated here with Google Earth imagery, showing that only three of the large trees have remained. Remaining farmland trees: 22 million; disappeared: 2.5 million (confidence >0.8). Basemap in **a** from Natural Earth (<https://www.naturalearthdata.com/>). Credit: **c,e**, Google Earth; **d**, Planet Labs PBC.

Azadirachta indica, *Madhuca longifolia*, *Acacia nilotica*, *Dalbergia sissoo*, *Syzygium cumini*, *Sesbania grandiflora*, *Albizia procera*, *Artocarpus heterophyllus* and *Cocos nucifera*, provide a variety of ecosystem services related to environmental conservation (for example, soil fertilization, shade) and products used for consumption (for example, fruits, fuelwood, fibre, mulch, medicine, fodder) or the generation of income (for example, wood, sap, medicine, fibre)^{7–10}. Agroforestry trees in India consist of remnant trees from forests (for example, *Madhuca longifolia*) that were left when land was cleared for agriculture but also include cultivated species (for example, *Cocos nucifera*). India is well known as a globally leading nation regarding the large-scale implementation of agroforestry and even urban systems⁷. However, the systematic quantification of tree resources within these systems is challenging at a national scale¹¹, and current mapping approaches capture mainly block plantations but fewer individual trees on farms¹¹. India has the largest agricultural area cover in the world, which makes tree cover and count in India uncertain and possibly one of the most overlooked woody elements globally.

Agroforestry trees can experience substantial temporal dynamics in their populations as they grow in highly managed ecosystems where some trees may be planted and others removed. The monitoring of these trees has become fundamental over the past decade,

not only to quantify available resources but also to identify possible climate-related diebacks, as observed in forests¹. A prominent example of a tree grown on farms is the Neem tree (*Azadirachta indica*), which can grow tall, with canopies of up to 20 m in diameter, and live up to several hundred years¹². Recent newspaper reports indicate that thousands of Neem trees in India have been infected by fungi over the past years, possibly leading to diebacks, which had already been identified as a potential problem several decades ago^{13,14}. Fungi, such as *Phomopsis azadirachtae*, attack old trees in particular while younger trees are stronger and survive the fungal infections. Pathogens/diseases are among the risks to trees intensified by global change, and fuelled by the synergistic effects of climate change and shifts in agricultural practices, among other social–environmental factors¹⁵. Due to the large number of trees at the national scale, it is a challenge to inventory them for a single year or repeated on an annual basis, and the extent of mortality from diseases, climate or human disturbances remains largely unknown.

Previously it has not been possible to study changes in scattered non-forest trees over time at a large scale. Individual trees that grow scattered in farmlands can be mapped from sub-metre-resolution satellite imagery, but these are not available as time series over larger areas, such as the country of India, and thus cannot be used for quantifying

dynamics at the level of individual trees in agricultural fields¹⁶. Satellite systems with a spatial resolution coarser than 10 m (for example, Sentinel 2) can detect groups of trees but not support detection of individual trees. The RapidEye archive is an often overlooked resource of satellite imagery, providing global coverage from micro-satellites back to August 2008. Together with PlanetScope (starting 2017), these satellite constellations provide a unique opportunity of repeated global coverage with images at a spatial resolution of 3–5 m, which allows the identification of individual trees^{17,18}. We have developed a heatmap-based tree-detection approach^{19,20} and deployed the RapidEye and PlanetScope satellite constellations to study changes in farmland trees at the individual tree level in India between 2010 and 2022.

Results

For this study, we map adult trees that can be identified as individuals within farmlands at a spatial resolution of 3–5 m. The spatial resolution of the imagery applied impedes the detection of small trees and limits the study to larger trees, typically with a crown size >10 m². Farmlands were delineated by a previously published state-of-the-art land-cover map (10 m resolution)⁵. This includes trees in fallow fields, hedgerows and trees along rural roads and rivers but excludes recently planted trees, which are not detectable in our images (Methods). Groups of trees and perennial plantations that form larger closed canopies, such as palm and rubber trees, are typically classified as ‘tree cover’ in the baseline land-cover map and are masked out in our study. Dense tree plantations can be part of agroforestry systems but are highly managed and include a high temporal dynamic from harvest and replanting, which makes this type of land use less relevant for this study, which is aiming at detecting longer-term changes in old farmland trees related to disturbances rather than recurrent management practices.

We formed country-wide custom generated mosaics of high-quality satellite scenes for each year 2010–2011 (RapidEye) and 2018–2022 (PlanetScope) and trained two deep-learning tree-detection models: one for RapidEye and one for PlanetScope, respectively. We merged the results from 2010 and 2011, and from 2018–2022, to ensure robustness in particular towards variations in image quality (Methods). The tree crown centres of individual trees mapped in 2010 or 2011 were tracked, and equivalents were identified during 2018–2022 (Fig. 1a,b). We used a buffer area of 15 m around the tree centre to account for potential spatial shifts in satellite image pairs. If a tree centre mapped in 2010 or 2011 was not found in one of the annual images between 2018 and 2022, it was counted as disappeared (Fig. 1b). When developing the models, we aimed for a very low false positive rate from the 2010/2011 detections (3%), meaning that only very few misclassifications exist. This method is tailored towards accurately detecting the disappearance of large trees and consequently is not designed for a wall-to-wall mapping of all individual trees in 2010/2011 as it may miss small trees. Therefore, we did not attempt to quantify the gain of small trees and net changes over the full period of analysis. We use the crown size to determine the size of a tree, which includes a considerable uncertainty at tree level²¹.

For the 2010–2018 change, we focused on trees that were detected with a high confidence (>0.8) in the RapidEye period (Methods) as these are typically large trees that are clearly identifiable, such as the Neem tree. This means that the instances of detection and changes reported are reliable but conservative and implies that the real numbers are probably higher. As a result, we refrain here from reporting absolute numerical values of change in number of trees. Results show that $11 \pm 2\%$ of the high-confidence trees mapped in 2010 or 2011 were not detected in the 2018–2022 images (Fig. 1). The 2% uncertainty was quantified by a manual checking of 1,000 random samples. We found that trees detected by RapidEye with a confidence >0.8 have an average crown size of 96 m² (Methods), which implies that the trees covered by this analysis were generally mature trees that have reached a later stage of development, and such a high loss rate of mature trees over less

than a decade is unexpected. The disappearance of mature farmland trees was observed in many areas, but numbers rarely exceed 5–10%, except for areas in central India, in particular in the states Telangana and Maharashtra, where we document massive losses of large trees (Fig. 1). Here several hotspot areas have lost up to 50% of their large farmland trees, with up to 22 trees per square kilometre disappearing (Fig. 1c–e). Smaller hotspot areas of loss are also observed, such as in eastern Madhya Pradesh around Indore (Extended Data Fig. 1).

We then focused on the period 2018–2022, where higher-quality PlanetScope imagery was further used for annual wall-to-wall tree detections (Fig. 2), although the detection reliability for small trees with a crown area below 10–20 m² is relatively low (Extended Data Table 1 and Methods). We mapped about 0.6 billion trees within the land-cover classes of cropland, urban and bare. The average number of trees per hectare is 0.6 (s.d. 1.6), and the highest densities are found in northwest (Rajasthan) and south-central India (Chhattisgarh), with up to 22 trees per hectare. We then tracked individual trees during 2018–2022. The condition was that a tree that was detected in either 2018 or 2019 with a high confidence and was not detected in the three consecutive years 2020–2022 was classified as disappeared, which ensures that the tree had actually disappeared and did not simply fail to be detected. We developed a metric termed ‘change confidence’, which quantifies the certainty to which a given tree actually disappeared (Methods). We focus exclusively on reporting tree losses accompanied by a high change confidence (>0.7). This approach acknowledges that the real figures may surpass those presented here, while intentionally omitting fluctuations of smaller trees and losses of trees characterized by considerable uncertainty in their reported numbers. We find that 5.3 million trees (2.7 trees per square kilometre) observed in 2018/2019 were not detected in 2020–2022. Trees with a change confidence above this threshold have an average crown size of 67 m². The uncertainty in the number of disappeared trees was 21%, quantified by manually checking a random sample of 1,000 trees classified as disappeared. This number of disappeared trees, considered a conservative estimate due to the method applied, was still high considering that a majority of the losses must have occurred between 2018 and 2020. Several hotspot areas stand out. The example shown in Fig. 3b–d is not a local exception from the rule, as we observed similar situations all over Indian croplands, reflecting a considerable national-scale thinning of India’s large farmland trees over such a short period. Some regions have lost more than 50 trees per square kilometre.

A potential driver of tree losses is climate change, with rapid increases in temperature in central and southern India²² and unfavourable trends in rainfall and drought conditions over the past decade (Extended Data Fig. 3a–c). However, compared with the long-term mean precipitation, the past decade was above average for most areas²³ (Extended Data Fig. 2d), and there is little evidence supporting climatic changes as the direct and main reason for the observed losses. We thus conducted qualitative interviews with villagers from the Telangana, Haryana, Kerala, Maharashtra, Andhra Pradesh, Uttar Pradesh, Kashmir and Jammu provinces, all affected by the disappearance of trees in our maps (Fig. 1). All participants in the interviews verified the considerable reduction in the populations of mature trees within and along fields. These trees were removed owing predominantly to alterations in the cultivation practices. The establishment of new boreholes, which resulted in an augmented water supply, facilitated the expansion of paddy rice fields with the objective of boosting crop yields. The decision to remove trees within fields is often driven by the perception that their benefits are relatively low and concerns that their shading effect, in particular for trees with a very large crown such as Neem trees, may adversely affect crop yields. While all interviewees reported that native trees within fields have become rare, several report that block plantations have increased. Fungi and climate were not perceived to have had an impact on tree populations by the interviewees.

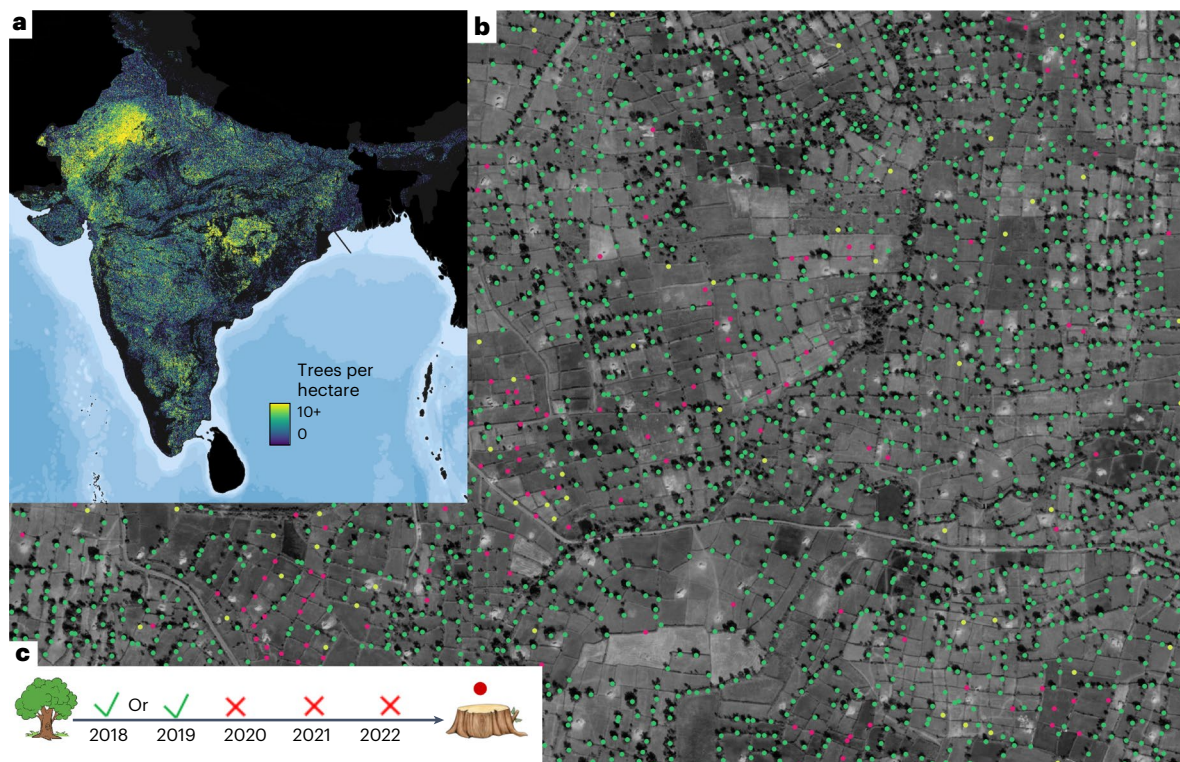


Fig. 2 | Presence of agroforestry trees during 2018–2022. **a**, Every tree within farmlands, urban areas and bare areas was mapped, and their density is shown here summed at the hectare scale. **b**, A demonstration of the framework to map the dynamics of individual trees in different agroforestry systems. Disappearance of trees can be caused by natural factors, part of management practices or related to disturbances, depending on the agroforestry type. The

basemaps are from Google Earth, 2021. **c**, A tree that was detected in either 2018 or 2019 (or both) with a high confidence but was not found in three consecutive years (2020–2022) was mapped as disappeared, shown here as red points. Number of mapped trees: 597,638,431. See Extended Data Fig. 2 for an illustration of the workflow. Basemap in **a** from Natural Earth (<https://www.naturalearthdata.com/>). Credit: **b**, Google Earth.

Discussion

The outcome of this study is twofold. First, we provide a tool that enables the monitoring of every individual large tree every year at a sub-continental scale (Extended Data Figs. 2 and 4–6). The imagery employed is not free of charge, but the cost is orders of magnitude lower than conventional sub-metre imagery¹⁷. We developed a deep-learning-based method that can be trained with simple point labels, which can be rapidly optimized for regional use^{19,20,24–26}. The database not only provides a complete inventory of mature farmland trees, but also offers the opportunity to locate and quantify trees that have disappeared. The database includes detection confidence values for each year 2018–2022. If a tree that has been detected with a high confidence (above a given threshold) is not detected anymore over several consecutive years, there is a high probability that the tree has disappeared. By combining the confidence values of each year, a change confidence can be derived, quantifying the uncertainty of whether a tree has disappeared or not. In this study, we refrained from making statements on low or medium confidence changes to take a conservative approach to the reporting of losses, but the dataset will be open for various applications. The database can be updated on an annual basis and scaled to global scale, potentially being a tool to support scientists, agroforestry practitioners, land managers and policymakers. Potential applications beyond inventorying are the monitoring of illegal logging of trees and the monitoring of survival rates of restoration areas. As a potential for future research, the spectral information could be used to study changes in the health of trees.

Second, our study reveals a concerning trajectory, documenting a considerable depletion of large farmland trees over the past decade in parts of India. This finding is particularly unsettling given the current emphasis on agroforestry as an essential natural climate solution,

playing a crucial role in both climate change adaptation and mitigation strategies, as well as for livelihoods and biodiversity^{27–31}. A certain loss rate is natural, and the cutting of trees is also part of agroforestry management systems, and not every lost tree is related to climatic disturbances or human appropriation, just as not every mapped tree contributes to livelihoods of local communities. There are also large areas in India where observed losses do not exceed expected dynamics. Nonetheless, an observable trend is emerging in several areas where established agroforestry systems are replaced with paddy rice fields³², which are being expanded and intensified³³, a development facilitated by the availability of newly established water supplies. Large and mature trees within these fields are removed, and trees are now being cultivated within separate block plantations typically with lower ecological value.

At a first glance, this may contradict official reports and recent studies stating that tree cover in India has increased considerably in recent years^{34,35}. It is, however, important to note that we report only gross losses and did not consider tree gains as a separate class. We also masked out block plantations. We thus cannot provide information on net tree changes, and our results do not contradict reports concluding that there has been a net increase in planted trees outside forests as a result of tree planting being encouraged and actively carried out in India. However, newly planted trees do not always contribute to biodiversity³⁶, and it can take a long time until they efficiently contribute to livelihoods. It is also unclear how newly planted trees survive in times of climate change. In light of the vast scale of global forest mortality caused by recent wildfires and droughts, the figures presented here may appear relatively modest, yet the substantial loss of particularly large farmland trees is disconcerting as virtually every large tree that has been lost may impact the ecosystem and, in the long term, the well-being and sustenance of communities.

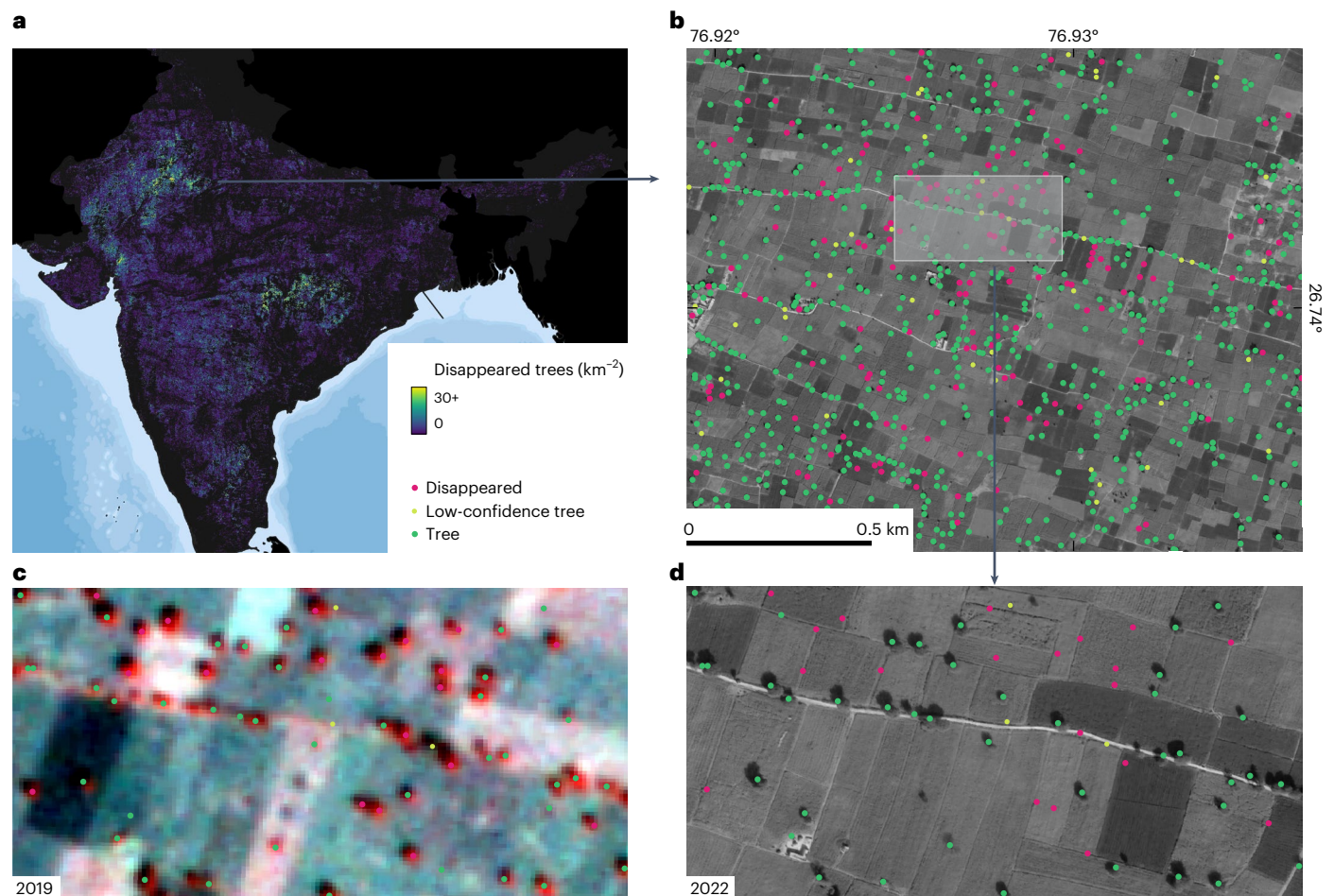


Fig. 3 | Disappearance of farmland trees 2018–2022. **a**, We estimate that 5.6 million trees have disappeared between 2018/2019 and 2020–2022, here shown per square kilometre. **b**, Zoom to a hotspot area in northwestern India where a substantial part of large farmland trees have disappeared over recent years. The arrow shows the location of the area within India. **c**, A PlanetScope scene captured in 2019, where trees classified as disappeared are still alive. The scene is shown as a false colour composite with near infrared as red colour,

causing tree crowns to appear in reddish colours. The rectangle in **b** marks the location. **d**, A considerable number of the trees detected in 2019 are not present anymore in 2022, visualized here with a Google Earth basemap. The crown sizes of the disappeared trees here are $>150\text{ m}^2$ (manually measured on the screen), which means trees were mature. Basemap in **a** from Natural Earth (<https://www.naturalearthdata.com/>). Credit: **b,d**, Google Earth; **c**, Planet Labs PBC.

The expansion and intensification of agriculture can lead to the simplification of natural and cultural landscapes³⁷, resulting in the loss of biodiversity³⁸, depletion of carbon reservoirs³⁹ and disappearance of indigenous knowledge on the ecological functioning of agroforestry systems. However, and despite receiving limited attention, diverse and complex multifunctional landscapes are still maintained by indigenous peoples and smallholders⁴⁰. According to the last census, more than 86% of the farmers in India are smallholder farmers with less than 2 hectares of land (and more than 67% of farmers less than 1 ha)⁴¹, in which trees may play an important role in their livelihoods⁴². Our results will be freely available, thereby inviting the research community to seize this opportunity for fieldwork and in-depth investigation to address existing uncertainties in agroforestry dynamics.

Methods

This study generates country-wide custom mosaics for RapidEye for 2010 and 2011 (5 m resolution) and for PlanetScope (3 m resolution) for 2018, 2019, 2020, 2021 and 2022. We trained deep-learning models to detect individual non-forest trees for each year and studied changes between years by tracking the tree crown centre over the years (Extended Data Figs. 2 and 4–6). We calculated a change confidence for each tree, which is composed of a multi-year detection confidence to

be able to quantify the uncertainty of the detection and of the change. The 2010/2011 maps detected mostly larger trees, but differences in image quality impeded exhaustive wall-to-wall mapping. The newer maps available after 2018 provide a more spatially consistent mapping of all farmland trees; however, the mapping was designed to exclude dense plantations and small/young trees. We did not set a strict height or crown-size threshold for the Planet data analysis, but a previous study has shown that trees below 4 m in height and with a crown size below 10 m^2 are likely not to be detected¹⁷ and that trees with crown sizes above 20 m^2 can be mapped with a relatively high confidence. Hence, comparing the 2010 maps with the 2018–2022 maps gives an overview of the disappearance of large trees, while the tracking of trees during 2018–2022 includes all trees that have reached a certain crown size, excluding newly planted trees.

Monitoring trees at the level of individuals over time requires consistency in high-quality images and reliable tree-detection methods. While this would be easier to address by using sub-metre imagery, these data are not available as time series over large areas. Imagery from nano-satellites is available at 3–5 m resolution at a high temporal frequency, but the quality of the images captured from several hundred different satellites varies substantially. This concerns in particular the image sharpness, and smaller trees will not be visible in images that

are blurred: a type of information that is not obvious from the scene metadata. Imagery at this spatial resolution is not suitable for pixel-wise stacking as image composites due to variations in the viewing angle. What is most important for the detection of trees is sharpness, and most other aspects, such as the number of spectral bands, can be neglected. Our solution to this issue was to filter each downloaded scene for sharpness using a blur kernel²⁶, and if a certain threshold was not reached, the image was blacklisted and the area was filled with different images until the threshold was passed.

The method used for the tree detection in this study diverges from previous deep-learning-based approaches^{16,17}. Studying changes at tree level at a continental scale requires a highly accurate and robust detection method that works over a variety of satellite images and landscapes. Here we developed a heatmap-based detection method^{19,20,43} that can be quickly trained with a large amount of point labels and is able to separate adjacent tree crowns reliably. The applied data are globally available, which makes our method widely applicable beyond the scope of farmland trees in India.

Image preparation

The RapidEye constellation was operational from 2009 to 2019 and consisted of five nano-satellites. The spatial resolution is 5 m, and the spectral bands are red, green, blue, red edge and near infrared. The PlanetScope constellation consists of 130+ nano-satellites with a resolution of 3–4 m and red, green, blue and near-infrared bands. We formed custom 1° x 1° mosaic tiles, each consisting of about 30 scenes for RapidEye and about 120 scenes (Dove Classic) or 60 scenes (Super Dove) for PlanetScope¹⁷. A histogram-matching algorithm with Landsat and Sentinel 2 scenes from the same period was applied for each tile to adjust differences in colours and form a homogeneous mosaic. The images were acquired following a phenological window derived from the Moderate Resolution Imaging Spectroradiometer phenology product (MOD09): For areas with deciduous trees, determined by the GlobCover map, images were acquired from the period between ‘senescence’ and ‘mid-greendown’. This particular period was selected as it represents the period after herbaceous vegetation has passed its productivity peak, whereas trees still have green leaves, facilitating the detection of tree crowns. For areas with evergreen trees, images were acquired between the mid-greendown and the ‘dormancy’, which is a period where herbaceous vegetation is not productive, but trees have full green leaves. If too few images were available meeting this criteria, we progressively extended the length of the time window until a maximum of 60 days was reached. If too few images were still to be found, we loosened the filtering criteria, allowing progressively lower ‘visible-confidence-percent’ values down to 60 to be included. We applied strict filtering criteria to use only images that are entirely free of clouds and have a low sun elevation (below 50), which facilitates the identification of trees by their shadow. The ground sample distance (GSD) of PlanetScope images varies between 3.1 and 4.7 m; we retained only images that have a GSD close to 3.1 m and never used imagery with a GSD above 4 m.

The identification of small trees is possible only in sharp images, and since there is a large variation in image sharpness between scenes that cannot be seen in the metadata, we applied a blur kernel to estimate the sharpness of the scene directly after download. The blur kernel is described in ref. 26, and we followed their recommendation to set a threshold of 0.23. We disregarded all scenes below this threshold and redownloaded the areas until the scene was classified as sharp. We applied the blur kernel only in images where the forest, shrubland, water, bare soil and wetland classes accounted for less than 50% of the scene coverage as the calculation of the blurriness score was found to be unreliable over these land-cover classes.

Since there is no reliable metadata on cloud cover in RapidEye images, we calculated the standard deviation for each downloaded scene and disregarded all scenes where the blue band had a very high

standard deviation, which is typically the case in cloudy images. This did not guarantee fully cloud-free images but, together with the blur kernel, removed most of the contaminated scenes.

The entire framework was automated and the filling of a 1° x 1° tile required about 2–3 hours using a university connection, but it can be performed in a parallelized way so the downloading, filtering and processing of one year requires less than one week for all India. All processing was done locally, and the raw data for one year is about 2.5 terabytes. As a final step, we applied a contrast limited adaptive histogram equalization to each mosaic and normalized the bands to values between 0 and 255 (ref. 44).

Training data

We manually labelled trees with point labels at the tree crown centre, using separate models for PlanetScope (about 130,000 labels) and RapidEye (about 100,000 labels), including labels from all years. For each labelled tree, we used high-resolution images in Google Earth and Bing to verify whether the trees existed. A large number of sub-metre images around 2010 were available from Bing maps and were used to verify labels from RapidEye, while Google Earth images were from recent years and used to verify labels from PlanetScope images. The labels were generated as an iterative process. In the first round, labels were generated over a variety of landscapes and image conditions (different viewing angles, sharpness levels and so on), being spatially well distributed across India. Then a first model was trained and trees were predicted over the study area. Subsequently, labels were added in areas where the performance was not satisfying, according to a visual inspection, and this process was repeated until the result was visually satisfying.

Trees are more challenging to map in RapidEye images at 5 m (6.5 m ground sample distance) as compared with PlanetScope data. They become clearly visible if they cover four pixels, which would translate to a crown size of >100 m². To reduce the number of false positives in our classification, we did not aim at a wall-to-wall mapping of trees in RapidEye images in 2010, but instead opted for a very low misclassification rate. Consequently, we labelled only clear examples, resulting in some heterogeneity in the tree maps (related to image quality, remaining cloud cover, sun elevation and visibility of the trees), generating a sample set of trees from 2010 with a certain randomness. By adding a second year, 2011, the combined results became more spatially consistent and homogeneous.

Tree detection

To produce the most reliable assessment of tree densities, we adapted a detection approach previously used to count dense objects, such as persons in a crowd. Our method is inspired by previous work^{19,20,43} and uses convolutional neural networks (CNNs) to produce a confidence map indicating the location of individual trees (Extended Data Fig. 6). The peak of the confidence map (‘heatmap’) is assumed to be the centre of a tree crown (Extended Data Figs. 2 and 5). The advantage of this method over previous methods^{16,17} is that it can be trained by point labels, which enables a rapid generalization and adjustment over large areas and different scene quality levels.

Heatmap-based detections typically transform discrete point labels into continuous Gaussian kernels, more suited to smooth optimization. It requires deciding on a fixed kernel scale, which is not straightforward here given the high level of variability in tree sizes, image quality and potential offsets between labelled and actual tree centres. A previous work²⁴ proposed a solution with adaptive kernels, where the model is given a degree of freedom through a scale map that resizes the Gaussian kernels on the fly during training. They also weigh the regression loss to focus on misestimated pixels, similarly to the Focal loss²⁵. Here we applied the same method, with two important modifications: we removed the linear approximation used originally and instead drew exact Gaussian kernels on the fly, and we allowed

only scale factors >1 , with a minimum standard deviation of 4.5 m for PlanetScope and 5 m for RapidEye. We found that these adjustments led to smoother heatmaps with fewer artefacts, which ultimately made it easier to tune the important hyperparameters of scale regularization and base Gaussian standard deviation (6 m for PlanetScope, 6.7 m for RapidEye).

We trained the models over 2,500 epochs, with a learning rate of 1×10^{-5} until epoch 2000, after which we used a linearly decreasing learning rate. The training process was monitored using 20% of the training data as validation data. We trained five models with different semi-random splits of the training data. After creating a list of possible random training and validation splits with an 80/20 proportion of the number of labelled areas, we selected splits that had a low Wasserstein distance between the distribution of trees per area in the training and validation sets. With a relatively high number of labelled areas (918 for PlanetScope, 791 for RapidEye), it ensures a diversity of training areas in the different models, while avoiding performance issues from unbalanced training and validation sets. The F1 scores on the heatmaps for all models ranged between 0.63 and 0.65 for a close radius of 20 m, and between 0.67 and 0.69 for a wider radius of 50 m (precision 0.83, recall 0.61 for 50 m), which is close to the values from ref. 19, although they used aerial images of higher spatial resolution. We then predicted on the mosaics using an ensemble over the five models and averaged the results of the heatmaps. The local maxima of the ensemble heatmap were converted to a point file, reflecting the centres of tree crowns. The peak confidence at the crown centre was saved as an attribute value associated with each centroid, reflecting the detection confidence. All peaks with a confidence equal to or above 0.35 were included in the following analyses. If the confidence was below 0.35, we considered this as no tree being detected.

A previously published tree crown segmentation model¹⁷ was updated with 52,000 manually drawn crown labels from India, and a tree crown segmentation was conducted for the year 2021 (Extended Data Fig. 4). Although this method is less reliable than the heatmap-based detection, it provides an overview of the crown-size distribution of the trees. Results showed that trees with a crown size below 20 m² were under-detected (Extended Data Table 1). We further located 22.7 million large trees with a crown size >100 m², which matches with the number of high-confidence trees detected by RapidEye in 2010/2011 (22 million; confidence >0.8). Note that trees with a crown size >50 m² or >100 m² represent only a small fraction of the woody populations, with proportions of about 20% and 4%, respectively (Extended Data Table 1).

We sampled trees from the heatmap predictions for the same area from both PlanetScope ($n = 2.1$ million) and RapidEye ($n = 1.2$ million) for 2019 (where RapidEye was still operational). We used the tree crown segmentation to determine the tree crown sizes of the point predictions from both PlanetScope and RapidEye by overlaying the tree crown segments with the point predictions and associating the crown area as an attribute to the points. We found that the average tree crown size of the samples was 55 m² from PlanetScope and 62 m² from RapidEye. Trees detected with a confidence >0.8 had an average crown size of 96 m² for RapidEye. For PlanetScope, trees with a confidence >0.7 had a crown size of 67 m²; for <0.7 , the crown size was on average 59 m². This gives evidence that a higher confidence value also indicates a larger crown size.

Mapping tree changes

This study focuses on tree losses rather than gains as new trees are typically not growing large over a few years, and consequently they would not be detected in a reliable way. Moreover, the 2010 classification did not allow for wall-to-wall mapping.

We developed a framework that via crown centre detection can track individual trees over an arbitrary number of temporal steps. We defined a circular buffer area of 15 m around the centre of a detected

tree and searched for centroid equivalents over the following images/years. If no tree was detected within the buffer area in the later years, the tree was counted a loss. If several trees were detected within the buffer, the closest tree was chosen.

For the long-term comparison between the early and late epoch, we combined the results from RapidEye (2010 and 2011) to reflect the early period and those of PlanetScope (2018–2022) to reflect the later period. Tree crown centres found in the early period were then compared with the later period, and a tree was classified either as disappeared, which means it was observed only in 2010/2011 but not during the later period, or as remaining, which means the tree was observed in both periods.

For the tracking of trees over the period 2018–2022, we developed a metric we named change confidence, which quantifies the confidence of our tree detection into the following three classes: disappeared, tree, and low-confidence tree/misclassification. A tree was marked as a low-confidence tree if it was detected in only one year with a low or medium confidence. The detection may be due to a misclassification or to the tree being too small to be reliably monitored over several years and was thus only detected in one year, so it was not included in the reported statistics. A centroid was marked as ‘tree’ if a tree was detected in one year with a very high confidence or in several years with a low or medium confidence. We marked a tree as disappeared if it was detected in either 2018 or 2019 with a high confidence, or in both years with a medium confidence, and then was not detected in three consecutive years (2020, 2021 and 2022). Mapping of disappearing trees and remaining trees with a low change confidence (<0.7) should be treated with caution. For example, if a tree mapped during 2018–2022 was mapped only in 2018 with a confidence of 0.5, it is likely that the tree is small or a false detection. If the tree is mapped only in 2018 with a confidence of 1.0, it is likely that the tree was then lost, as it was not mapped during 2019–2022. This assumes that a tree with a high confidence is a large tree that should be detected at least twice over 5 years. By contrast, if a tree was mapped with a lower confidence of 0.5 in 2018, but also in 2021 and 2022, the class is tree and the overall change confidence is higher as the tree was detected in 3 years, which reduces the risk of a misclassification.

Sources of uncertainties

Our change confidence metric quantifies uncertainty at tree level. Focusing only on trees with a high change confidence reduces the uncertainty of the change instances reported, but misses a number of cases of change that are real—but where the confidence is low due to image quality issues or the tree having a small crown. There are, however, a number of remaining sources of uncertainty that are challenging to quantify.

A tree was counted as disappeared during 2018–2022 only if the combined confidence of 2018 and 2019 was above 0.7 and the tree was not detected between 2020 and 2022. While this gives a certain robustness, we observed cases where the image quality was excellent in both 2018 and 2019 resulting in very high-confidence predictions, but the image quality was less ideal in all subsequent years 2020–2022, so some trees were missed in these three years, causing trees to be falsely classified as being disappeared. To account for this, we assumed that high-quality images in general generate higher confidence predictions compared with lower-quality images, so we calculated the average detection confidence of all trees within 1×1 km cells as a measure of image quality for each particular cell, which also accounts for quality variations within images. We then calculated a linear slope through the 1×1 km confidence grids, with time as the independent variable. A strong negative slope (<-0.05) implies that the average confidence in 2020–2022 was considerably lower than in 2018–2019, so we flagged this area as uncertain, and losses were not included in our reported numbers. The confidence slope map represents an additional layer

(to the change confidence) that quantifies uncertainty that we provide with the database.

Some RapidEye scenes are spatially shifted, which leads to erroneous classifications of tree losses. When comparing the 2010/2011 results with the 2018–2022 results, we calculated the proportion of trees disappearing for each RapidEye scene footprint. If the proportion was above 40%, scenes were probably shifted and we masked them. We also manually masked scenes that were clearly shifted, visible by sharp edges along footprints.

A final source of uncertainty that cannot be quantified is the land-cover map included in our analysis. We used the WorldCover map from 2020 to retain only croplands for the 2010–2018 comparison, and cropland, urban and bare for the 2018–2022 comparison. The quality of the land-cover map impacts the results, and it happens that large farmland trees or groups of trees are masked out as forest or that the underlying classification is not correct. Future versions may include custom land-cover maps, which may lead to improved results. Using a land-cover map from 2020 to study changes over 10 years can include areas that have been cleared for cropping and have not previously been farmland, or were under fallow, or plantation forest. However, we observed that these areas rarely included large trees but rather shrubs and small trees, and by reporting mainly the loss of high-confidence trees, these are automatically excluded.

Evaluation of the tree detections and changes

We randomly selected 1,000 points mapped as disappeared trees between 2010/2011 and 2018–2022 to evaluate the uncertainty on the reported long-term losses. The same 1,000 points were used to evaluate whether trees were correctly mapped in 2010/2011 or whether it was a false detection. We further selected 1,000 random trees that had been mapped as disappeared trees over 2018–2022 to evaluate the uncertainty related to disappeared trees over the PlanetScope period. Each point was manually and visually checked on the images and in Google Earth, also using the historic images where available. For the losses, we considered only high-confidence changes, with values above 0.8 for RapidEye and 0.7 for PlanetScope. Uncertainties would be higher if different confidence thresholds were used. False detections of trees for 2010/2011 were found to be 3%. False losses for 2010–2018 were 2%. False losses for 2018–2022 were 21%.

We further conducted 12 qualitative interviews with villagers in the Telangana, Haryana, Kerala, Maharashtra, Andhra Pradesh, Uttar Pradesh, Kashmir and Jammu provinces during August 2023. The interviews were about 20–60 minutes each, and we asked about soils, management systems, water resources, changes in the number of trees and possible reasons for changes. Participants were on average 59 years old. We explained our research briefly before conducting the interviews. We informed participants that we would use the information to understand the dynamics of large agroforestry trees. All interviewees accepted and provided answers to all questions.

Reporting summary

Further information on research design is available in the Nature Research Reporting Summary linked to this article.

Data availability

The data can be viewed online at <https://rs-cph.projects.earthengine.app/view/tree> and are available via Zenodo at <https://zenodo.org/records/10978154> (ref. 45).

Code availability

A similar tree-detection framework is available in ref. 19. The crown segmentation framework is available via Zenodo at <https://doi.org/10.5281/zenodo.3978185> (ref. 46). A similar framework including both segmentation and counting can also be found at <https://github.com/sizhuoli/TreeCountSegHeight>. A simplified version

of the PlanetScope mosaic generation is available via Zenodo at <https://doi.org/10.5281/zenodo.7764360> (ref. 47).

References

- Allen, C. D. et al. A global overview of drought and heat-induced tree mortality reveals emerging climate change risks for forests. *For. Ecol. Manage.* **259**, 660–684 (2010).
- Senf, C., Buras, A., Zang, C. S., Rammig, A. & Seidl, R. Excess forest mortality is consistently linked to drought across Europe. *Nat. Commun.* **11**, 6200 (2020).
- Hammond, W. M. et al. Global field observations of tree die-off reveal hotter-drought fingerprint for Earth's forests. *Nat. Commun.* **13**, 1761 (2022).
- Terasaki Hart, D. E. et al. Priority science can accelerate agroforestry as a natural climate solution. *Nat. Clim. Change* **13**, 1179–1190 (2023).
- Zanaga, D. et al. ESA WorldCover 10 m 2020 v100. *Zenodo* <https://doi.org/10.5281/zenodo.5571936> (2021).
- Taylor, J. R. & Lovell, S. T. Designing multifunctional urban agroforestry with people in mind. *Urban Agric. Reg. Food Syst.* **6**, e20016 (2021).
- Chinnamani, S. Agroforestry research in India: a brief review. *Agrofor. Syst.* **23**, 253–259 (1993).
- Basu, J. P. Agroforestry, climate change mitigation and livelihood security in India. *N. Z. J. For. Sci.* **44**, S11 (2014).
- Dinesha, S. & Teli, S. B. Millet-based agroforestry: a nature-positive farming to achieve climate-resilience and food security in India and Africa. *SSRN* <https://doi.org/10.2139/ssrn.4461034> (2023).
- Johar, V. Socio-economic and environmental assets sustainability by agroforestry systems: a review. *Int. J. Agric. Environ. Biotechnol.* **14**, 521–533 (2021).
- Rizvi, R. et al. *Mapping Agroforestry and Trees Outside Forest* (World Agroforestry, 2020); <https://www.worldagroforestry.org/publication/mapping-agroforestry-and-trees-outside-forest>
- Islas, J. F. et al. An overview of neem (*Azadirachta indica*) and its potential impact on health. *J. Funct. Foods* **74**, 104171 (2020).
- Bhat, S. S., Sateesh, M. K. & Devaki, N. S. A new destructive disease of neem (*Azadirachta indica*) incited by *Phomopsis azadirachtae*. *Curr. Sci.* **74**, 17–19 (1998).
- Nagendra Prasad, M. N., Shankara Bhat, S., Charith Raj, A. P. & Janardhana, G. R. Detection of *Phomopsis azadirachtae* from dieback affected neem twigs, seeds, embryo by polymerase chain reaction. *Arch. Phytopathol. Plant Prot.* **42**, 124–128 (2009).
- Singh, B. K. et al. Climate change impacts on plant pathogens, food security and paths forward. *Nat. Rev. Microbiol.* **21**, 640–656 (2023).
- Brandt, M. et al. An unexpectedly large count of trees in the West African Sahara and Sahel. *Nature* **587**, 78–82 (2020).
- Reiner, F. et al. More than one quarter of Africa's tree cover is found outside areas previously classified as forest. *Nat. Commun.* **14**, 2258 (2023).
- Spiekermann, R. *Change of Woody Vegetation and Land Cover Using High Resolution Images on the Dogon Plateau and Sèno Plains (Mali)* (Univ. Vienna, 2013).
- Ventura, J. et al. Individual tree detection in large-scale urban environments using high-resolution multispectral imagery. Preprint at <https://doi.org/10.48550/arXiv.2208.10607> (2022).
- Li, S. et al. Deep learning enables image-based tree counting, crown segmentation, and height prediction at national scale. *PNAS Nexus* **2**, pgad076 (2023).
- Mugabowindekwe, M. et al. Nation-wide mapping of tree-level aboveground carbon stocks in Rwanda. *Nat. Clim. Change* **13**, 91–97 (2023).
- Mishra, V. & Aadhar, S. Famines and likelihood of consecutive megadroughts in India. *NPJ Clim. Atmos. Sci.* **4**, 59 (2021).

23. Jin, Q. & Wang, C. A revival of Indian summer monsoon rainfall since 2002. *Nat. Clim. Change* **7**, 587–594 (2017).
24. Luo, Z. et al. Rethinking the heatmap regression for bottom-up human pose estimation. In *Proc. 2021 IEEE/CVF Conference on Computer Vision and Pattern Recognition (CVPR)* 13259–13268 (IEEE, 2021); <https://doi.org/10.1109/CVPR46437.2021.01306>
25. Lin, T.-Y., Goyal, P., Girshick, R., He, K. & Dollár, P. Focal loss for dense object detection. *IEEE Trans. Pattern Anal. Mach. Intell.* **42**, 318–327 (2020).
26. Anger, J., de Franchis, C. & Facciolo, G. Assessing the sharpness of satellite images: study of the planetscope constellation. In *Proc. IGARSS 2019—2019 IEEE International Geoscience and Remote Sensing Symposium* 389–392 (IEEE, 2019); <https://doi.org/10.1109/IGARSS.2019.8900526>
27. Singh, P. et al. Agroforestry improves food security and reduces income variability in semi-arid tropics of central India. *Agrofor. Syst.* <https://doi.org/10.1007/s10457-023-00806-6> (2023).
28. Telwala, Y. Unlocking the potential of agroforestry as a nature-based solution for localizing sustainable development goals: a case study from a drought-prone region in rural India. *Nat. Based Solut.* **3**, 100045 (2023).
29. Karlson, M. et al. Exploring the landscape scale influences of tree cover on crop yield in an agroforestry parkland using satellite data and spatial statistics. *J. Arid. Environ.* **218**, 105051 (2023).
30. Skole, D. L., Mbow, C., Mugabowindekwe, M., Brandt, M. S. & Samek, J. H. Trees outside of forests as natural climate solutions. *Nat. Clim. Change* **11**, 1013–1016 (2021).
31. Datta, P. & Behera, B. in *Strategizing Agricultural Management for Climate Change Mitigation and Adaptation* (ed. Bandh, S. A.) 167–181 (Springer, 2023); https://doi.org/10.1007/978-3-031-32789-6_10
32. Han, J. et al. Annual paddy rice planting area and cropping intensity datasets and their dynamics in the Asian monsoon region from 2000 to 2020. *Agric. Syst.* **200**, 103437 (2022).
33. Akula, M., Bandumula, N. & Rathod, S. Rice production in Telangana: growth, instability and decomposition analysis. *Oryza* **59**, 232–240 (2022).
34. Fagan, M. E. et al. The expansion of tree plantations across tropical biomes. *Nat. Sustain.* **5**, 681–688 (2022).
35. Du, Z. et al. A global map of planting years of plantations. *Sci. Data* **9**, 141 (2022).
36. Edwards, D. P. et al. Upscaling tropical restoration to deliver environmental benefits and socially equitable outcomes. *Curr. Biol.* **31**, R1326–R1341 (2021).
37. Foley, J. A. et al. Global consequences of land use. *Science* **309**, 570–574 (2005).
38. Estrada-Carmona, N., Sánchez, A. C., Remans, R. & Jones, S. K. Complex agricultural landscapes host more biodiversity than simple ones: a global meta-analysis. *Proc. Natl Acad. Sci. USA* **119**, e2203385119 (2022).
39. Sanderman, J., Hengl, T. & Fiske, G. J. Soil carbon debt of 12,000 years of human land use. *Proc. Natl Acad. Sci. USA* **114**, 9575–9580 (2017).
40. Fernández-Llamazares, Á. et al. Scientists' warning to humanity on threats to indigenous and local knowledge systems. *J. Ethnobiol.* **41**, 144–169 (2021).
41. *Agriculture Census* <https://agcensus.gov.in/AgriCensus/> (Ministry of Agriculture and Farmers Welfare, 2024).
42. Reang, D. et al. Piper agroforestry in the Indian Himalayas: indigenous peoples' practices, policies and incentives. *CABI Agric. Biosci.* **5**, 9 (2024).
43. Osco, L. P. et al. A convolutional neural network approach for counting and geolocating citrus-trees in UAV multispectral imagery. *ISPRS J. Photogramm. Remote Sens.* **160**, 97–106 (2020).
44. Zuiderveld, K. in *Graphics Gems IV* 474–485 (Academic Press, 1994).
45. Brandt, M. et al. Farmland trees in India (2018–2022). *Zenodo* <https://doi.org/10.5281/zenodo.10978154> (2024).
46. Kariryaa, A. An-unexpectedly-large-count-of-trees-in-the-western-Sahara-and-Sahel. *Zenodo* <https://doi.org/10.5281/zenodo.3978185> (2020).
47. Reiner, F. download_planet. *Zenodo* <https://doi.org/10.5281/zenodo.7764360> (2023).

Acknowledgements

M.B., F.R., W.Z. and X.T. are supported by the European Research Council (ERC) under the European Union's Horizon 2020 research and innovation programme (grant agreement no. 947757 TOFDry). M.B. also acknowledges funding from a DFF Sapere Aude grant (no. 9064–00049B). A.K. and R.F. acknowledge support by the Villum Fonden through the project Deep Learning and Remote Sensing for Unlocking Global Ecosystem Resource Dynamics (DeReEco).

Author Contributions

M.B. designed the study, prepared the data, sampled the training data, trained the models, conducted the analyses, designed the figures and wrote the manuscript. F.R. wrote the codes for the data preparation and data analyses, supported by X.T. D. Gominski wrote the codes for the tree-detection framework. The importance of the contributions of M.B., F.R. and D. Gominski can be considered as equal. A.K. and V.B.G. conducted the interviews. W.Z. analysed the climate data. P.C., R.F., D.O.-G. and D. Govindarajulu reviewed the manuscript.

Competing interests

The authors declare no competing interests.

Additional information

Extended data is available for this paper at <https://doi.org/10.1038/s41893-024-01356-0>.

Supplementary information The online version contains supplementary material available at <https://doi.org/10.1038/s41893-024-01356-0>.

Correspondence and requests for materials should be addressed to Martin Brandt, Dimitri Gominski or Florian Reiner.

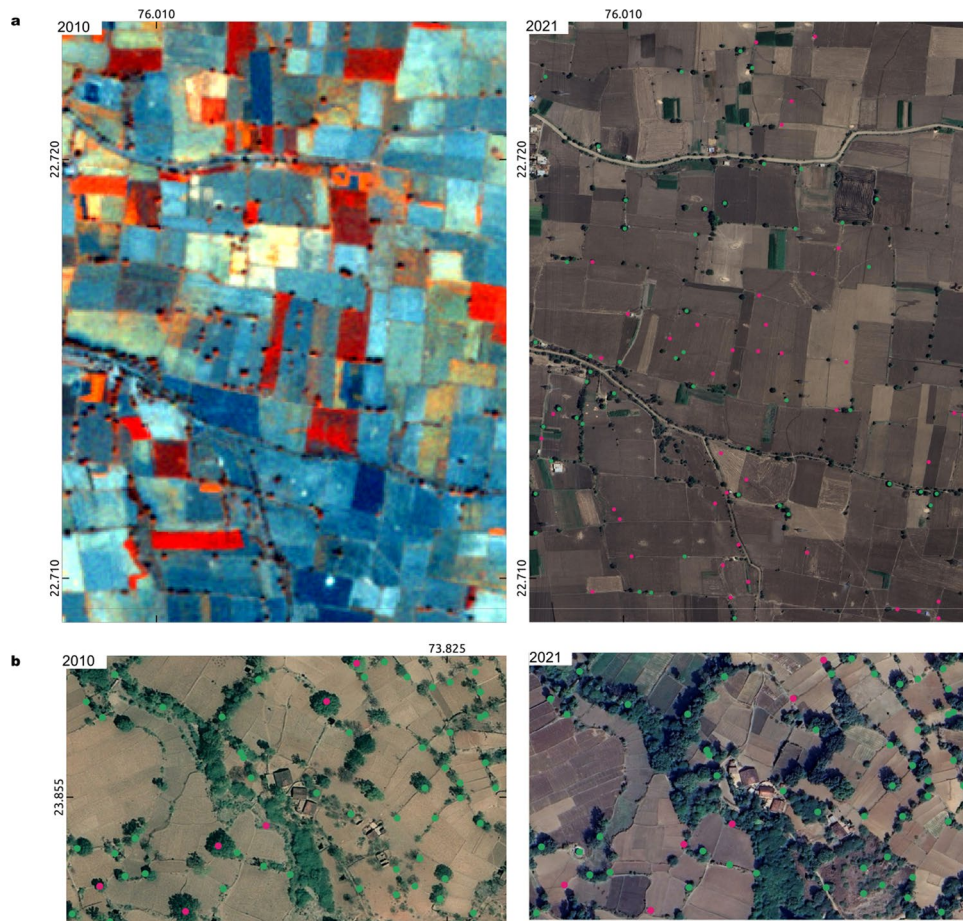
Peer review information *Nature Sustainability* thanks Martin Karlson, Arun Jyoti Nath and Lucas Prado Osco for their contribution to the peer review of this work.

Reprints and permissions information is available at www.nature.com/reprints.

Publisher's note Springer Nature remains neutral with regard to jurisdictional claims in published maps and institutional affiliations.

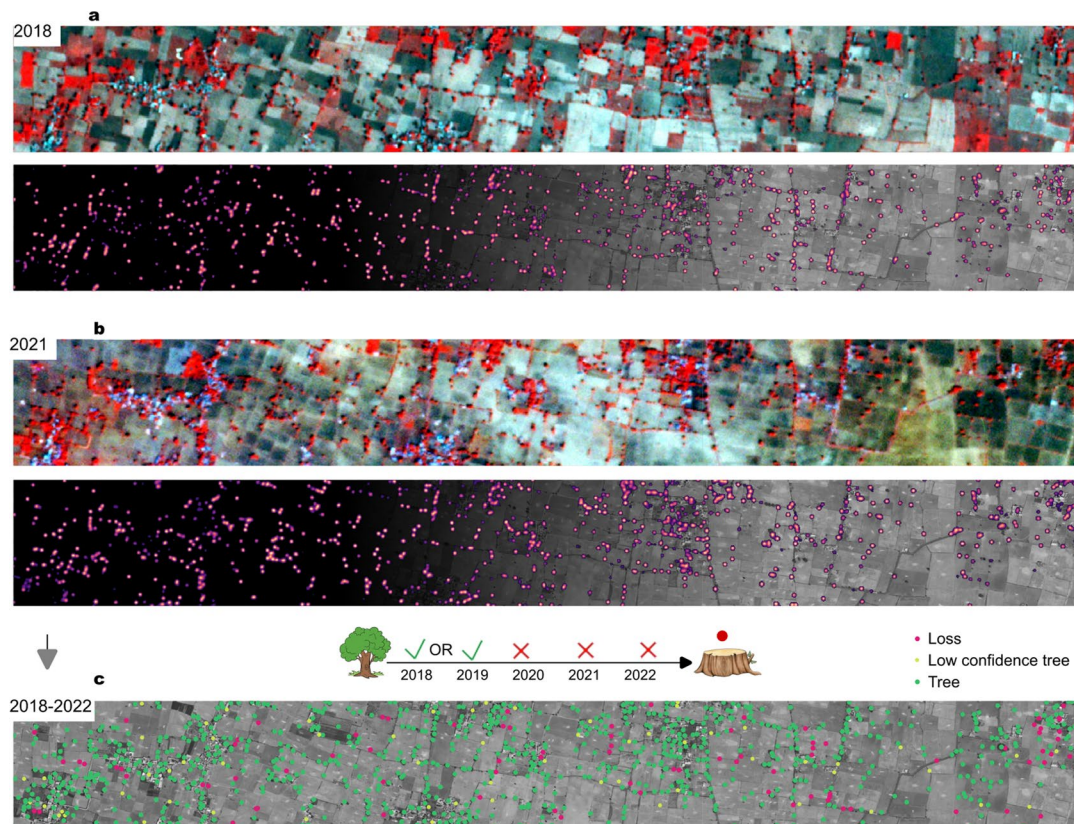
Open Access This article is licensed under a Creative Commons Attribution 4.0 International License, which permits use, sharing, adaptation, distribution and reproduction in any medium or format, as long as you give appropriate credit to the original author(s) and the source, provide a link to the Creative Commons licence, and indicate if changes were made. The images or other third party material in this article are included in the article's Creative Commons licence, unless indicated otherwise in a credit line to the material. If material is not included in the article's Creative Commons licence and your intended use is not permitted by statutory regulation or exceeds the permitted use, you will need to obtain permission directly from the copyright holder. To view a copy of this licence, visit <http://creativecommons.org/licenses/by/4.0/>.

© The Author(s) 2024



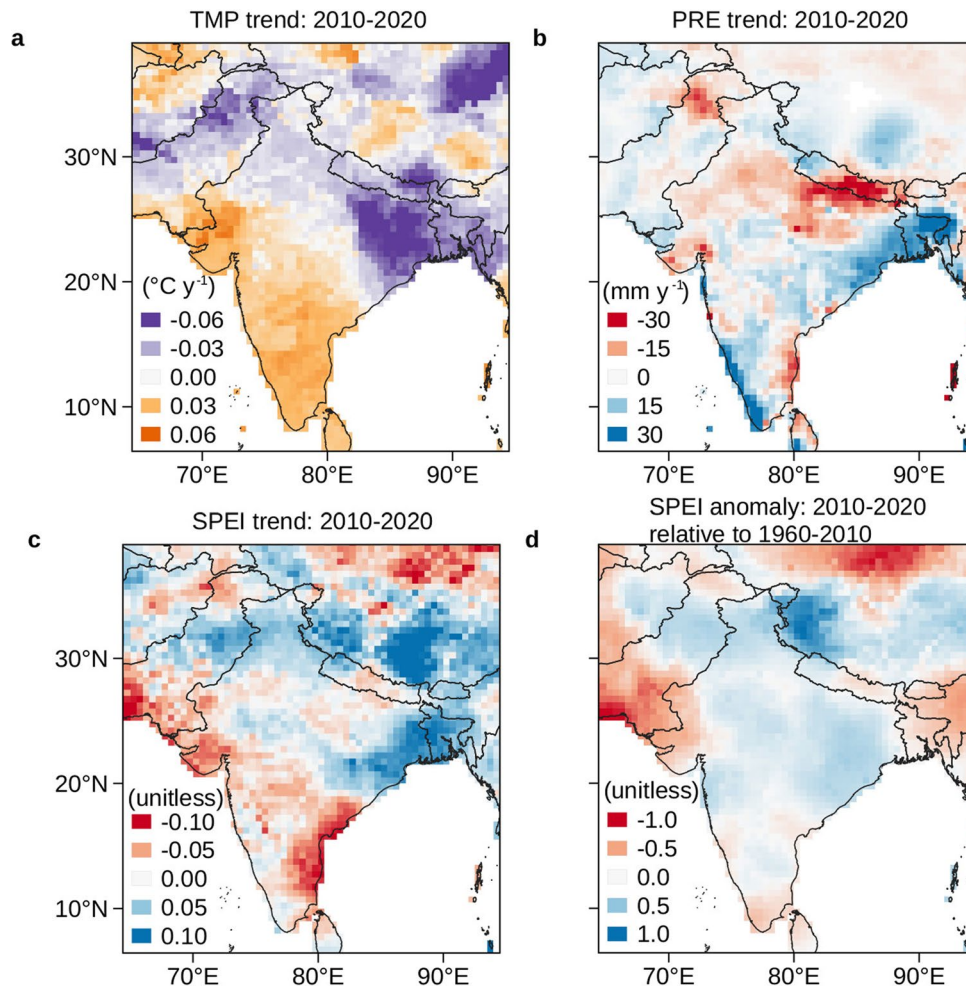
Extended Data Fig. 1 | Examples of tree losses 2010–2018. **a**, The lefthand side shows a RapidEye false color composite from 2010, the righthand side shows the area in 2021 illustrated in Google Earth. The red points are trees mapped in 2010,

that are not present anymore during 2018–2022. Green points are trees mapped both in 2010 and 2018–2022. **b**, Close-up showing the disappearance of several very large trees. Credit: **a**, Planet Labs PBC; **b**, Google Earth.



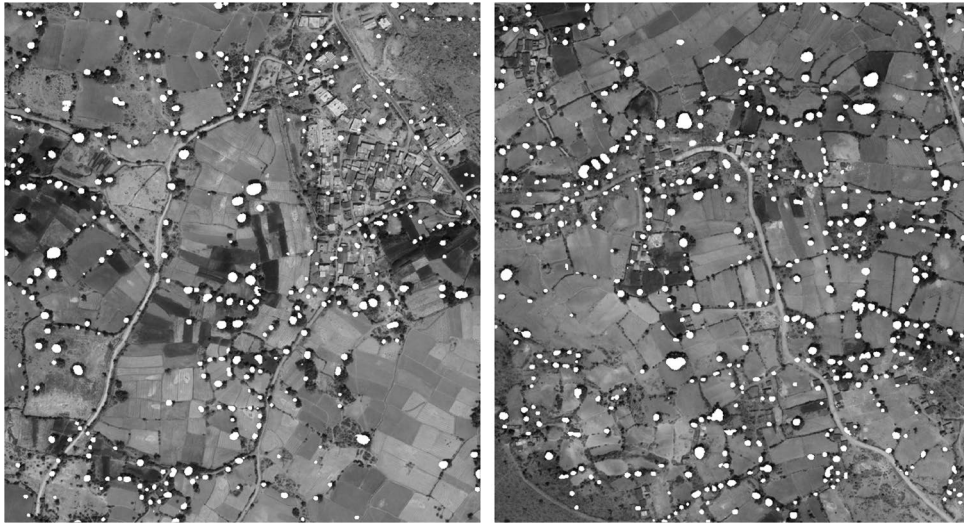
Extended Data Fig. 2 | Detecting change at tree level. a, A PlanetScope scene from 2018 shown as a false color composite with NIR shown as red color, causing tree canopies and active fields to appear in reddish colors. We trained a deep learning model with point labels and predicted a heatmap, reflecting the confidence values of the predictions. The local maxima of the heatmap were extracted as points, reflecting the location of tree crown centers. The detection confidence was saved as an attribute value associated with each point.

b, The same as (a) but for 2021. c, The above-mentioned workflow was applied for 2018, 2019, 2020, 2021 and 2022. A tree that was detected with a high confidence in 2018 and/or 2019 but not in 2020, 2021 and 2022, was classified as a loss, otherwise as a tree. If the overall confidence over 5 years was in the range between 0.4–0.7, the tree was marked as a low confidence tree. Credit: **a, b**, Planet Labs PBC; **c**, Google Earth.



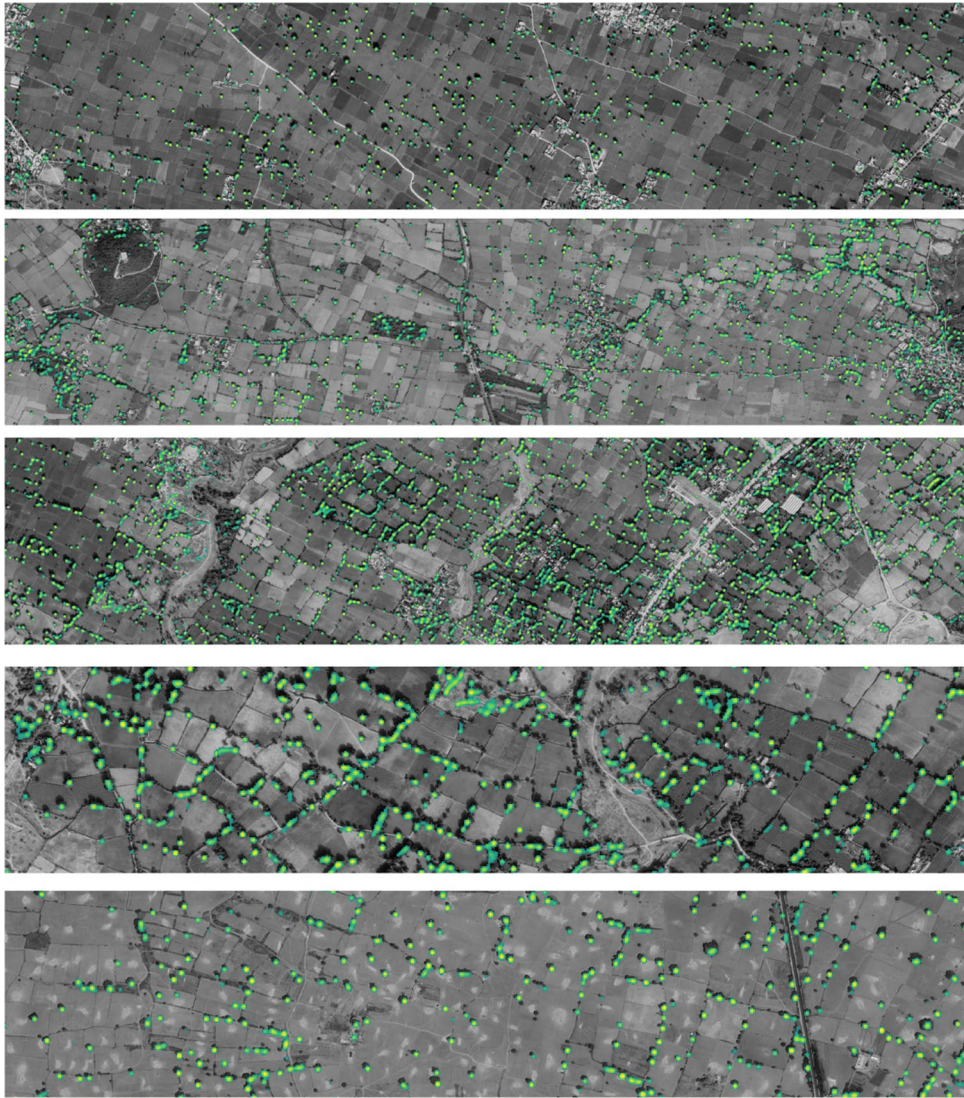
Extended Data Fig. 3 | Climate change in India. a, Trend in air temperature during 2010–2020. b, Trend in precipitation during 2010–2020. c, Trend in SPEI during 2010–2020. SPEI is a measure of drought, including both rainfall and

air temperature. Negative values reflect conditions that are unfavorable for vegetation growth. d, SPEI anomaly of the period 2010–2020 as compared to the long term mean 1960–2010.

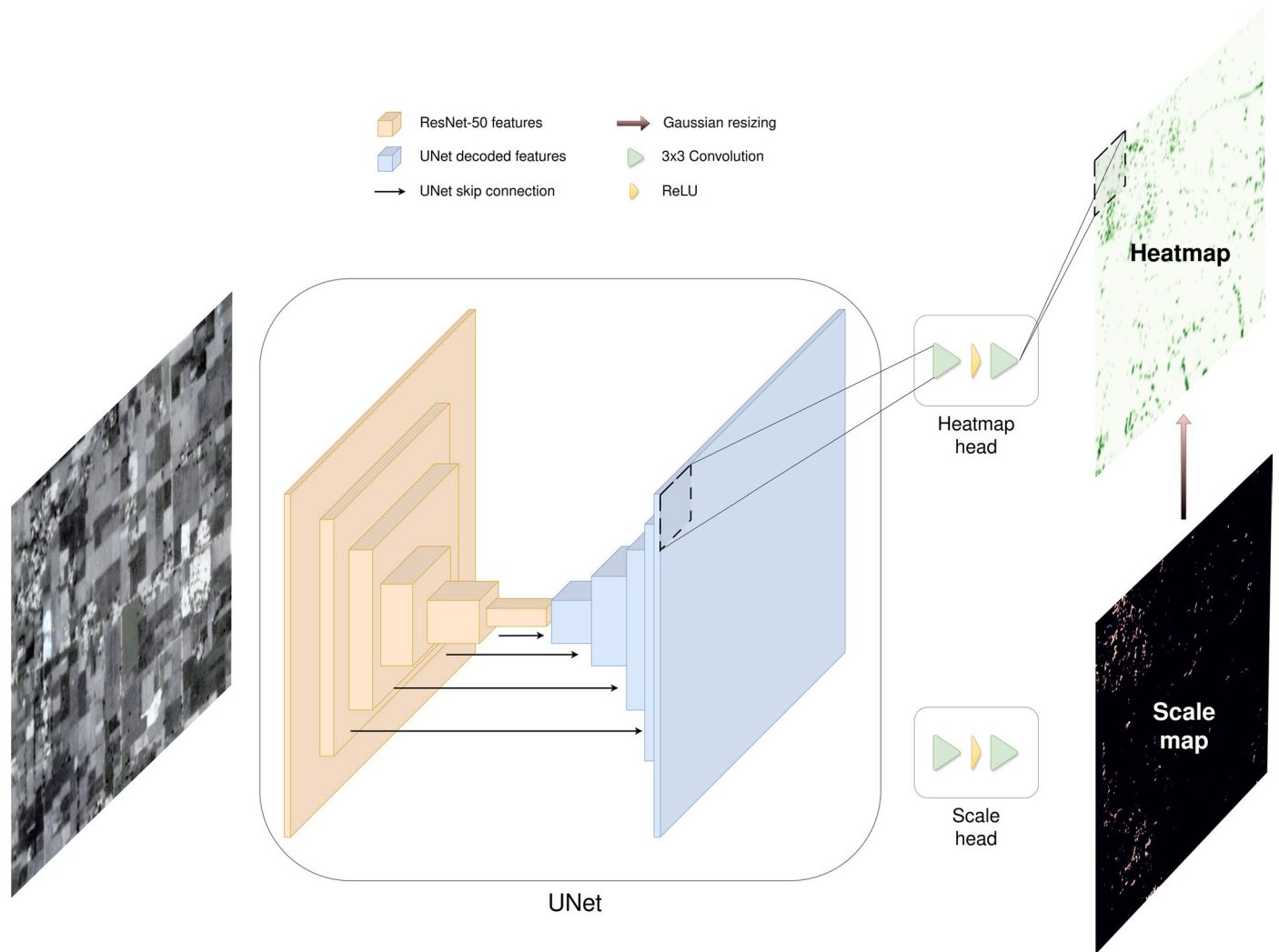


Extended Data Fig. 4 | Tree crown segmentation. We segmented tree crowns over all images, using a previously published model¹⁵ plus about 50,000 new labels. The results were not used for the temporal change analysis because the

heatmap-method has shown to be more robust. The segmentation gives however a good overview on the general distribution of tree crown sizes (Extended Data Table 1). Credit: Google Earth.



Extended Data Fig. 5 | Gaussian heatmaps. We predict heatmaps where the local maxima represent the tree crown centers. The heatmap itself can serve as a tree cover map with a precision down to each individual tree, and the size of the gaussian can be used to estimate the crown size, which was however not utilized in this study. This visualization uses different zoom levels. Credit: Google Earth.



Extended Data Fig. 6 | Model architecture. We use the UNet architecture with a ResNet-50 encoder and two custom heads, one predicting a heatmap indicating tree center confidence and the other predicting a scale map. The scale map is used during training to let the model resize the individual Gaussian kernels and make them fit visual features. Credit: of the greyscale image on the left: Google Earth.

Extended Data Table 1 | Tree crown segmentation for 2021

Crown area	0-5 m ²	5-20 m ²	20-50 m ²	50-100 m ²	100-200 m ²	200-300 m ²	>300 m ²
Count	36 millions	110 millions	314 millions	120 millions	21 millions	1.4 millions	0.3 millions

N=0.6 billion. See ref. 17 for details on the segmentation process.

Reporting Summary

Nature Portfolio wishes to improve the reproducibility of the work that we publish. This form provides structure for consistency and transparency in reporting. For further information on Nature Portfolio policies, see our [Editorial Policies](#) and the [Editorial Policy Checklist](#).

Statistics

For all statistical analyses, confirm that the following items are present in the figure legend, table legend, main text, or Methods section.

n/a Confirmed

- The exact sample size (n) for each experimental group/condition, given as a discrete number and unit of measurement
- A statement on whether measurements were taken from distinct samples or whether the same sample was measured repeatedly
- The statistical test(s) used AND whether they are one- or two-sided
Only common tests should be described solely by name; describe more complex techniques in the Methods section.
- A description of all covariates tested
- A description of any assumptions or corrections, such as tests of normality and adjustment for multiple comparisons
- A full description of the statistical parameters including central tendency (e.g. means) or other basic estimates (e.g. regression coefficient) AND variation (e.g. standard deviation) or associated estimates of uncertainty (e.g. confidence intervals)
- For null hypothesis testing, the test statistic (e.g. F , t , r) with confidence intervals, effect sizes, degrees of freedom and P value noted
Give P values as exact values whenever suitable.
- For Bayesian analysis, information on the choice of priors and Markov chain Monte Carlo settings
- For hierarchical and complex designs, identification of the appropriate level for tests and full reporting of outcomes
- Estimates of effect sizes (e.g. Cohen's d , Pearson's r), indicating how they were calculated

Our web collection on [statistics for biologists](#) contains articles on many of the points above.

Software and code

Policy information about [availability of computer code](#)

Data collection

Data analysis

For manuscripts utilizing custom algorithms or software that are central to the research but not yet described in published literature, software must be made available to editors and reviewers. We strongly encourage code deposition in a community repository (e.g. GitHub). See the Nature Portfolio [guidelines for submitting code & software](#) for further information.

Data

Policy information about [availability of data](#)

All manuscripts must include a [data availability statement](#). This statement should provide the following information, where applicable:

- Accession codes, unique identifiers, or web links for publicly available datasets
- A description of any restrictions on data availability
- For clinical datasets or third party data, please ensure that the statement adheres to our [policy](#)

The data can be viewed online at <https://rs-cph.projects.earthengine.app/view/tree> and is available for download via <https://zenodo.org/records/10978154>. Any usage must be solely for noncommercial education or scientific research purposes, and publication in academic or scientific research journals. Licensee agrees that all such publications must include an attribution that clearly and conspicuously identifies "PlanetLabs PBC" as the source of the content on which the publication was based.

Research involving human participants, their data, or biological material

Policy information about studies with [human participants or human data](#). See also policy information about [sex, gender \(identity/presentation\), and sexual orientation](#) and [race, ethnicity and racism](#).

Reporting on sex and gender	na
Reporting on race, ethnicity, or other socially relevant groupings	na
Population characteristics	na
Recruitment	na
Ethics oversight	na

Note that full information on the approval of the study protocol must also be provided in the manuscript.

Field-specific reporting

Please select the one below that is the best fit for your research. If you are not sure, read the appropriate sections before making your selection.

Life sciences Behavioural & social sciences Ecological, evolutionary & environmental sciences

For a reference copy of the document with all sections, see [nature.com/documents/nr-reporting-summary-flat.pdf](https://www.nature.com/documents/nr-reporting-summary-flat.pdf)

Ecological, evolutionary & environmental sciences study design

All studies must disclose on these points even when the disclosure is negative.

Study description	We use annual PlanetSope satellite data for 2018-2022 and RapidEye data from 2010 and 2011 to study the dynamics of trees in farmlands in India.
Research sample	The data used for this study consisted of 3 m, 4-band satellite imagery. The study area comprised India, but not forests which were masked out, as well as lakes and rivers which were excluded with a water mask. The images were obtained from Planet Labs via the NICFI program, with raw scenes downloaded via the Planet API and then merged together in 1 x 1 degree composite mosaics.
Sampling strategy	all trees in farmlands that have reached a certain size and are visible in the satellite image are included.
Data collection	Data was collected via the Planet API by Florian Reiner and Martin Brandt.
Timing and spatial scale	The daterange of each mosaic is specific to the phenology of that region, such that trees are in full foliage while interference from grasses is minimised. The years are 2010, 2011, 2018, 2019, 2020, 2021, 2022.
Data exclusions	Of all PlanetScope images available, scenes were filtered by date range (using the phenology-determined temporal window), and then by quality, using API filters such as percent clouds, haze and visual confidence. Of the selected scenes, only a subset is used to create a gapless mosaic, with the scene footprints being clipped before download to reduce redudant downloads.
Reproducibility	With the deep learning framework used, prediction of trees of a given mosaic is deterministic, i.e. predicting the same image several times will always give the same result.
Randomization	na
Blinding	na

Did the study involve field work? Yes No

Reporting for specific materials, systems and methods

We require information from authors about some types of materials, experimental systems and methods used in many studies. Here, indicate whether each material, system or method listed is relevant to your study. If you are not sure if a list item applies to your research, read the appropriate section before selecting a response.

Materials & experimental systems

n/a	Involvement in the study
<input checked="" type="checkbox"/>	<input type="checkbox"/> Antibodies
<input checked="" type="checkbox"/>	<input type="checkbox"/> Eukaryotic cell lines
<input checked="" type="checkbox"/>	<input type="checkbox"/> Palaeontology and archaeology
<input checked="" type="checkbox"/>	<input type="checkbox"/> Animals and other organisms
<input checked="" type="checkbox"/>	<input type="checkbox"/> Clinical data
<input checked="" type="checkbox"/>	<input type="checkbox"/> Dual use research of concern
<input checked="" type="checkbox"/>	<input type="checkbox"/> Plants

Methods

n/a	Involvement in the study
<input checked="" type="checkbox"/>	<input type="checkbox"/> ChIP-seq
<input checked="" type="checkbox"/>	<input type="checkbox"/> Flow cytometry
<input checked="" type="checkbox"/>	<input type="checkbox"/> MRI-based neuroimaging

Plants

Seed stocks

na

Novel plant genotypes

na

Authentication

na